Dynamic Walking on exoskeleton ATALANTE with virtual constraints regulation

Victor Paredes and Ayonga Hereid

Abstract— Control design for bipedal robots with hybrid zero dynamics provides stable gaits for 2D and 3D robots. However, 3D robots still pose a challenge to stabilize because there is no lateral stabilization control. It becomes even more challenging for exoskeletons because of the unmodelled dynamics of the user and forces the user excerts upon it. One of the most common methods to avoid falls in the HZD context are the use of regulators, i.e., heuristic controllers that aid the robot during walking. However, they lack formal stability guarantees as they change the designed HZD path. This paper proposes a ZMP based regulation for bipedal robots with feet; the regulator modifies the HZD outputs such that they can adjust the ZMP trajectory to keep the robot from falling while maintaining the hybrid invariance of the generated orbit.

I. INTRODUCTION

A study of the Christopher Dana Reeve Foundation states that nearly 1 in 50 people are living with paralysis in the United States [**?**]. Unfortunately, many people with lower-limb paralysis face tough challenges to mobilize and frequently need the assistance of a caregiver. Restoring their ability to walk or providing support during rehabilitation with lower-limb exoskeletons is a promising solution for improving their quality of life. Many lower-limb exoskeletons have been developed since earlier work in 1960 at the Mihalio Pupin Institute in Belgrade [1] and the University of Wisconsin [2] to this day [3]. Although those exoskeletons posses reliable hardware, their locomotion capabilities are limited by their walking and stability controllers: either they require the use of crutches for balance and direction or they provide static gaits with stability limitations.In consequence, exoskeletons require more efficient walking controllers that pose a better robustness performance for unmodelled dynamics that could originate a fall.

Bipedal walking design for robotics typically uses two paradigms: (1) relying on low-dimensional models [4]–[6], and (2) the exploitation of the full dynamics of the robot [7], [8]. Using low-dimensional models allows us to use simple expressions to calculate stability bounds or provide real-time solutions for planning gaits [9]. On the other hand, considering the full dynamics enables the robot to attain high efficiency and stable walking gaits as long as the states of the full system evolve along the generated stable limit cycle.

A very known stability parameter used on low-dimensional models is the so-called Zero Moment Point (ZMP), which enforces ground reaction forces being always inside the support foot [10], [11]. Those methods have the advantage of generating trajectories in real-time and using a stability criterion that is easily measured. Additionally, by using simplified models, the capture point method [12] computes bounds of stability to estimate the region where the robot needs to step to avoid a fall. Each different low-dimensional model presented capture more strategies and expand the region of stability as the model gains complexity.

On the other hand, limit cycle walkers were inspired by the observation that passive walkers exploit their full dynamics to generate a stable gait [13], highlighting a mathematical abstraction that enforces the periodicity and stability of the walking gaits. The stability of the limit cycle for actuated robots is achieved by enforcing a control law that renders the hybrid zero dynamics (HZD) invariant under the continuous dynamics, and the impact map generated the collision of the foot with the ground [7], [14].

The primary tool to generate walking gaits in the context of HZD is through nonlinear optimization by choosing an adequately set of constraints and periodicity conditions [15], [16] and obtain a phase-variable dependent trajectory used as a virtual-constraint for control design. One of the main benefits of the HZD method is the mathematical generalization to different types of robots and the efficiency exhibited by them [16]. Unfortunately, this method produces one walking trajectory, and deviations from it during experiments can break its stability with moderate ease.

Handling the problem of deviations from the nominal HZD trajectory requires further control action. For instance, heuristic control regulators are widely used to tune the gait until a reaching level of robustness as used in the robot Atrias [17] or Durus [16]; in those approaches, an optimization algorithm generates a set of virtual-constraints that are mathematically stable for an ideal model. However, for implementation, an additional control action was used as a foot-placement strategy to prevent the robot from rolling over its foot and fall. The action of this regulation works beyond the HZD method for the same robot, as it generates a stable walking gait for Atrias at different speeds [18], affirming its importance for robot walking.

A way to extend the application of the walking gaits generated through HZD is to switch among different limit cycles [19], providing behaviors such as stopping, running, turning, among others able to switch sequentially. Furthermore, it provides a way to increase the region of the stability of the robot since having several gaits can aid the robot to switch among them when there is a deviation from the nominal one

V. Paredes is with the department of Mechanical and Aerospace Engineering, The Ohio State University, OH 43210, USA `paredescauna.1@osu.edu`

A. Hereid is with the department of Mechanical and Aerospace Engineering, The Ohio State University, OH 43210, USA `hereid.1@osu.edu`

using interpolation or regression among orbits [17], [20] for example.

The manipulation of the HZD outputs [21], [22], also permits the generation of a new family of walking gaits that can exhibit different speeds with the advantage of keeping mathematical properties of stability of the original gait. For instance, Veer [21] proposed to add a term to the virtual-constraints calculated from the actual and the target speed using the jacobian of the forward speed. This term holds specific properties to conserve the hybrid invariance and stability of the original gait.

Since lateral stability is one of the main problems during 3D walking, we propose to use a similar procedure to Veer [21] to maintain the hybrid invariance of the walking gait. With this procedure and by relying on the ZMP criterion and the use of a low-dimensional model for the lateral movement of the robot, it is possible to provide a regulation that keeps the lateral ZMP under the support polygon to avoid a fall.

We propose a new regulation strategy for the lateral ZMP that produces a hybrid invariant orbit generated from the nominal, optimized HZD orbit. The main advantage of this regulator is its direct relationship with the ZMP as a stability criterion that can be measured and controlled.

With this goal for the paper, Sec. II starts with the mathematical formulation of the traditional hybrid zero dynamics approach, considering the exoskeleton model. The control design using virtual constraints and the optimization problem are discussed in Sec. III. Sec. IV presents the main contribution of the paper as it derives the mathematical expression and states the main theorem for the regulation on the virtual constraints. The results for both simulation and experiment are shown in Sec. V with details of the optimization problem, the computer running the simulation, and the gait results. Finally, in Sec. VI a discussion of the overall methodology is presented.

II. MATHEMATICAL FOUNDATIONS OF HYBRID ZERO DYNAMICS FRAMEWORK

This section presents a mathematical model for a powered lower-limb exoskeleton. In particular, we take into consideration the hybrid nature of bipedal locomotion and pose an optimization problem that considers impacts and looks for stable periodic behaviors by enforcing invariant reduced dimensional manifolds via virtual-constraint-based feedback controller. However the virtual constraints will be modified by an extra output used for CoM regulation which by construction do not disturb the hybrid invariance of the nominal gait generated through the HZD optimization.

A. Hardware Description

ATALANTE (Wandercraft, France) is a battery-powered lower limb exoskeleton designed to enable hand-free dynamic walking for individuals with paraplegia. It has a total weight of 75Kg and can be worn by a patient of up to 90Kg. Each leg of ATALANTE has six actuated joints, conformed by transversal hip, frontal hip, sagittal hip, sagittal knee, henke ankle, and sagittal ankle, as shown in
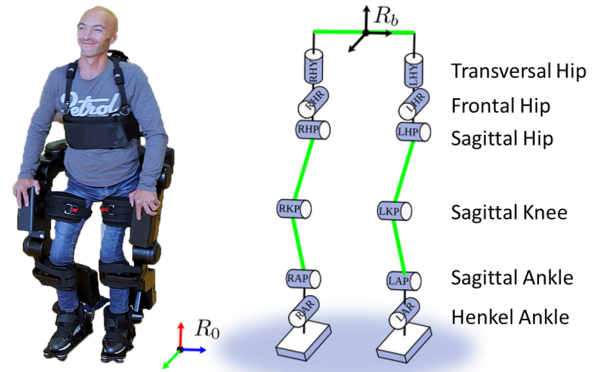

Fig. 1.   Kinematic representation of the exoskeleton ATALANTE exoskeleton.

Fig. 1. Among them, the henke and sagittal ankle joints are controlled through two differential linear actuators, and the rest are directly actuated with brushless DC motors through a harmonic drive. Each motor is commanded through an ELMO driver board, and the whole system is managed by a central computer running a real-time Linux system. For the control design in this paper, we will consider each joint as an independent rotational joint.

B. Robot Modelling

Because the exoskeleton is designed to fully support the user's weight, the user is securely strapped to the device from the feet up to the abdomen. To study the dynamical behavior of the human-exoskeleton and to avoid over-complicating the model by considering the compliant elements present in the human body and exoskeleton linkages, the lumped human-exoskeleton system is modeled as a rigid body hybrid dynamical system. Let R_b is a body-fixed reference frame attached at the pelvis link, $q_b \in \mathbb{Q}_b$ is the configuration of the actuated joints, p and ϕ are the position and orientation of the origin of R_b with respect to the world frame R_0, the configuration of the floating base coordinate system of ATALANTE is given by

$$q = (p, \phi, q_b) \in \mathbb{Q}, \tag{1}$$

with $\mathbb{Q} = SE(3) \times \mathbb{Q}_b$. Considering the presence of both continuous and discrete dynamics in bipedal locomotion due to the swing foot impacts with the ground, we use a hybrid dynamical system to represent the periodic walking of the exoskeleton. In this paper, we are interested in a flat-foot walking motion consisting of two phases, as shown in Fig. 2.

The walking of the human-exoskeleton system can be expressed as a hybrid control system ($\mathscr{HC}$) .

$$\mathscr{HC} = \{\Gamma, \mathscr{D}, \mathscr{U}, S, \Delta, FG\} \tag{2}$$

where Γ is the directed graph (e.g., Fig. 2), $\mathscr{D} \subset T\mathbb{Q}$ is a smooth manifold representing the admissible domain of the system states, $\mathscr{U}$ represents the admissible controls, $S \subset \mathscr{D}$ is the switching surface, Δ is the reset map, and FG represents the equations of motion of the continuous
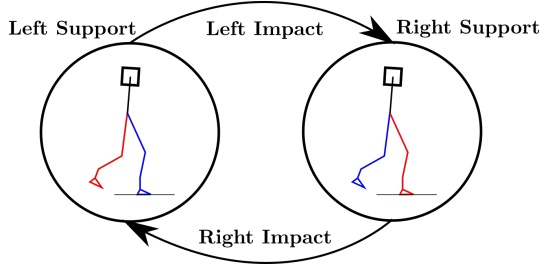
Fig. 2. A directed graph representing the flat foot walking phases for ATALANTE. We assume that at any moment there is only one support foot that lies flat on the ground.

dynamics. For more details regarding the construction of the hybrid system model, we refer the readers to [23], [24].

C. Hybrid Zero Dynamics based Feedback Controller

The idea of Hybrid Zero Dynamics is that if there exists a feedback tracking control $u \in \mathcal{U}$ that renders the hybrid system hybrid invariant, i.e., invariant through impacts, the full order dynamics to behave as a reduced dimensional system determined by the hybrid invariant orbits, termed hybrid zero dynamics (HZD) [7], [14]. This is realized by carefully designing a set of virtual constraints for the system.

The virtual constraints for the exoskeleton ATALANTE are defined as the difference between actual ($y^a(q)$) and desired outputs ($y^d(\tau(q), \alpha)$) and are (vector) relative degree 2, given by

$$y(q, \alpha) = y^a(q) - y^d(\tau(q), \alpha), \qquad (3)$$

where τ is a state-based phase variable used as a timing variable instead of time. Under an appropriate control law $u \in \mathcal{U}$ the virtual constraints are zeroed rendering the zero dynamics [14].

$$\mathscr{Z}_\alpha = \{(q, \dot{q}) \in \mathscr{D} | y(q, \alpha) = 0, \dot{y}(q, \dot{q}, \alpha) = 0\} \qquad (4)$$

A forward invariant zero dynamics manifold means that any state that starts in $\mathscr{Z}_\alpha$ remains in $\mathscr{Z}_\alpha$ until reaching the guard S. To render the zero dynamics invariant under impacts, the set of parameters α must be designed such that after the reset map (Δ) is applied, the states remain in $\mathscr{Z}_\alpha$.

$$\Delta(S \cap \mathscr{Z}_\alpha) \in \mathscr{Z}_\alpha \qquad (5)$$

Finding the set of parameters α is typically solved through a constrained nonlinear optimization problem [15], [16].

D. Gait generation

In this paper we use FROST to optimize a periodic walking gait for ATALANTE [15]. Let z contains all the optimization variables; the optimization problem can be stated as

$$z^* = \underset{z}{\operatorname{argmin}} \mathscr{L}(z) \qquad (6)$$

$$z_{min} \leq z \leq z_{max} \qquad (7)$$

$$c_{min} \leq c(z) \leq c_{max} \qquad (8)$$

The cost function ($\mathscr{L}$) is defined as

$$\mathscr{L} = \sum_{j=1}^{2} (\int_0^T ||u_j(\tau)||^2 d\tau + P(\dot{q}_j, u_j)) \qquad (9)$$

where $j \in 1, 2$ represents left and right leg support phase, $u_j(t)$ the control input for each phase, $P(\dot{q}_j, u_j)$ is the mechanical power of the gait and τ is the phase variable. The constraints in the optimization can be expressed as:

1) Physical Constraints: In addition to the stability constraints, other physical constraints must be considered in the optimization problem to generate a feasible gait for implementation in experiments. Characteristic hardware limitations include torque bounds, joint angle bounds, and velocity limits. Those constraints integrate into the optimization as bounds of the optimization variables in (7).

2) Design constraints: To generate human-like gaits, we use additional constraints that limit the solution space of the optimization into realistic bounds. For instance, the torso orientation must be upwards with reasonable movement bounds

$$\phi_{min}^{tor} \leq \phi^{tor}(z) \leq \phi_{max}^{tor} \qquad (10)$$

The swing foot must maintain a certain height during the step to avoid scuffing

$$h_{swing}(q) > 0 \qquad (11)$$

The swing foot must impact the ground with low negative velocity

$$-v_{max} \leq h'_{swing}(q, \dot{q}) \leq 0 \qquad (12)$$

The ground reaction wrench must be bounded and enforce the ZMP constraint

$$W_{min} \leq W(q, \dot{q}, u) \leq W_{max} \qquad (13)$$

The impact invariance condition (5) together with the design constraints are expressions of the optimization variables of the form (8).

III. REGULATION OF ZMP CONSTRAINTS

This section presents the mathematical formulation to regulate the ZMP through the virtual constraints maintaining the hybrid invariance associated with the optimized $\mathscr{Z}_\alpha$.

A. Regulation on Virtual Constraints

In this section the virtual constraints (3) will be augmented with and additional term $h_s(\tau(q), \beta)$ to allow changes on y_{CoM}. Consider the new virtual constraints $y_\beta(q, \alpha)$

$$y_\beta(q, \alpha) = y(q, \alpha) - h_s(\tau(q), \beta) \qquad (14)$$

$$y_\beta(q, \alpha) = y^a(q) - (y^d(\tau(q), \alpha) + h_s(\tau(q), \beta)) \qquad (15)$$

where $h_s(\tau, \beta) = B_M(\tau)\beta$ is the extra term, $B_M(\tau)$ is a Bezier polynomial and β a vector of parameters.

The new hybrid zero dynamics surface is $\mathscr{Z}_\beta$ and is defined as:

$$\mathscr{Z}_\beta = \{(q, \dot{q}) \in \mathscr{D} | y_\beta(q, \alpha) = 0, \dot{y}_\beta(q, \dot{q}, \alpha) = 0\} \qquad (16)$$

Note that when the states evolve on $\mathscr{Z}_\beta$ they are completely defined by:

$$y^a(q) = y^d(\tau, \alpha) + B_M(\tau)\beta \qquad (17)$$

$\mathscr{Z}_\beta$ deviates from $\mathscr{Z}_\alpha$ by the introduction of the additional term, to conserve the hybrid invariance property it must hold that the additional term $h_s(\tau, \beta)$ vanishes at the extremes points of $\mathscr{Z}_\beta$ as stated in [21].

Theorem 1. *If $\mathscr{Z}_\alpha$ is hybrid invariant, there exists a control law u_β that renders $\mathscr{Z}_\beta$ forward invariant and $h_s(\tau, \beta)$ meets condition 1) and 2), then $\mathscr{Z}_\beta$ is hybrid invariant.*

1) $h_s(\tau, \beta)$ *vanishes at the beginning and end of the gait.*

$$h_s(0, \beta) = h_s(T, \beta) = 0; \qquad (18)$$

2) $\frac{d}{d\tau}h_s(\beta, \tau)$ *vanishes and the beginning and end of the gait.*

$$h_s'(0, \beta) = h_s'(T, \beta) = 0; \qquad (19)$$

Proof: Note that the guard S is reached at the end of the step ($\tau = T$) and given condition 1) and 2) both $\mathscr{Z}_\alpha$ and $\mathscr{Z}_\beta$ coincide, as shown in Fig. 3, then:

$$x \in S \cap \mathscr{Z}_\alpha \to x \in S \cap \mathscr{Z}_\beta \qquad (20)$$

By condition of the theorem, $\mathscr{Z}_\alpha$ is impact invariant $\Delta(S \cap \mathscr{Z}_\alpha) \subset \mathscr{Z}_\alpha$ and together with (20) it leads to

$$\Delta(S \cap \mathscr{Z}_\beta) \subset \mathscr{Z}_\alpha \qquad (21)$$

At $\tau = 0$, by conditions 1) and 2) both $\mathscr{Z}_\alpha$ and $\mathscr{Z}_\beta$ will coincide as well (Fig. 3), then

$$\Delta(S \cap \mathscr{Z}_\beta) \subset \mathscr{Z}_\beta \qquad (22)$$

Revealing that $\mathscr{Z}_\beta$ is impact invariant. Since $\mathscr{Z}_\beta$ is forward invariant under u_β and impact invariant, then it is hybrid invariant.
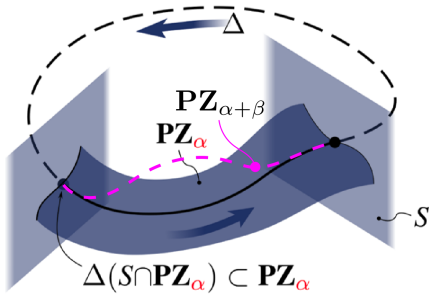
Fig. 3. The surfaces $\mathscr{Z}_\alpha$ and $\mathscr{Z}_\beta$ share the same guard and undergo the same reset map.

B. Lateral ZMP regulation

During experiments, ATALANTE presents lateral instability revealing that tracking the virtual-constraints does not guarantee stability. Some strategies to avoid falling use a foot-placement regulator based on the hip velocity of the robot or the torso orientation [16], [17], although the

new trajectories would not respect the behavior of the zero dynamics designed during the HZD optimization.

To work towards the goal of avoiding a fall, we note that a lateral fall implies a violation of the lateral ZMP during walking. Regulating the ZMP would prevent this issue, and by following the output construction in [21], the resulting regulation would maintain the hybrid invariance property while avoiding a fall.

By considering the movement of the robot as an inverted pendulum [10], we can simplify the ZMP into an equation that depends entirely on the center of mass (CoM) trajectory

$$y_{ZMP} = y_{CoM} - \frac{z_{CoM}}{g}\ddot{y}_{CoM} \qquad (23)$$

Since we are interested in regulating the lateral ZMP such that it lies on the support foot, we can change the ZMP location by a lateral movement of the center of mass. Assuming that the desired location of the lateral center of mass is $y^d{}_{CoM} = y_{CoM} + \Delta y_{CoM}$ and generates the desired location of the ZMP y^d_{ZMP}

$$y^d{}_{ZMP} = y^d{}_{CoM} - \frac{z_{CoM}}{g}\ddot{y}^d_{CoM} \qquad (24)$$

$$y^d{}_{ZMP} = y_{ZMP} + \Delta y_{CoM} - \frac{z_{CoM}}{g}\Delta\ddot{y}_{CoM} \qquad (25)$$

To produce a change in the lateral CoM, we can use a linear approximation dependent on the robot configuration q

$$\Delta y_{CoM} = \frac{\partial y_{CoM}}{\partial q}(q(\tau))\Delta q \qquad (26)$$

Assuming that the system is initially evolving on $\mathscr{Z}_\alpha$ and then switches to $\mathscr{Z}_\beta$ with states described by (17), we can express Δq as

$$\Delta q = B_M(\tau)\beta \qquad (27)$$

Using this expression onto (26) we obtain a relationship between Δy_{CoM} and β

$$\Delta y_{CoM} = \frac{\partial y_{CoM}}{\partial q}B_M(\tau)\beta = \Lambda(\tau)\beta \qquad (28)$$

Considering the relationship between the ZMP and the change on y_{CoM} (25),

$$\hat{y}_{ZMP} = y_{ZMP} + \Lambda(\tau)\beta - \Lambda''(\tau)\beta \qquad (29)$$

$$\hat{y}_{ZMP} - y_{ZMP} = (\Lambda(\tau) - \Lambda''(\tau))\beta = \Phi(\tau)\beta \qquad (30)$$

$$\beta^T = \Phi(\tau)^+(\hat{y}_{ZMP} - y_{ZMP}) \qquad (31)$$

where $\Phi(\tau)^+$ is the right inverse of $\Phi(\tau)$ and behaves as weighting vector, in the case of ATALANTE it assigns more weight over the frontal hip in the supporting leg which leads to torso roll movements.

IV. SIMULATION AND EXPERIMENTAL RESULTS

In this section, we present details of the implementation of the controller on the robot ATALANTE, given its capabilities as well as the simulation and experimental results of the proposed approach.
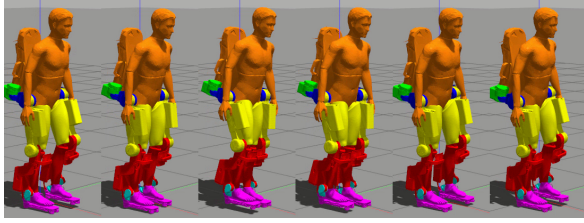
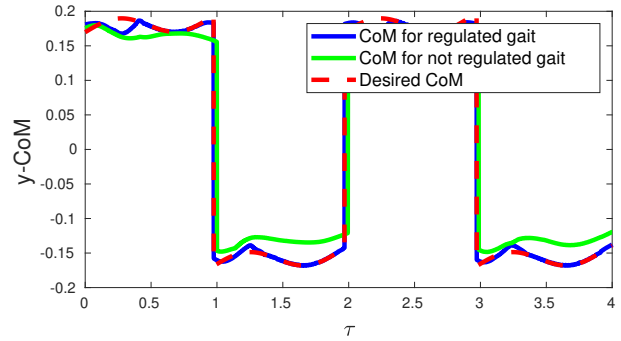Fig. 4.   Simulation of ATALANTE using CoM regulation (32)

Fig. 5.   Comparison of CoM trajectories for regulated and unregulated walking. Upper curve is for right leg support and lower curve for left leg support.

A. Implementation Details

Since ATALANTE does not have force sensors to measure ZMP it is not possible to implement direct ZMP regulation (31), instead we will drive back the actual CoM trajectory $y_{CoM}(q)$ to the designed trajectory $y_{CoM}(\tau)$ using (28). Considering (28), the parameter β can be calculated as:

$$\beta^T = B_M(\tau) \left(\frac{\partial y_{CoM}}{\partial q} \right)^+ (y_{CoM}^d - y_{CoM}^a) \qquad (32)$$

where $\left(\frac{\partial y_{CoM}}{\partial q} \right)^+$ represents the right inverse and $y_{CoM}^d(\tau)$ is calculated from $\mathscr{Z}_\alpha$.

The optimization problem is solved using hereid2017frost in MATLAB for two walking domains using a direct collocation scheme with 10 nodes for each domain and the Hermite-Simpson interpolation. The selected step time is 1s, and the forward hip velocity is 0.05 m/s, which is a comfortable speed for users using the exoskeleton.

As there is no force sensor information available on the feet, a current-based algorithm detects the impact with the ground whenever the current passes a threshold. The resulting switching times range from 0.7 to 0.8s (70%-80%) for both simulation and experiment.

B. Simulation Results

This section provides the simulation of the walking gait and the performance of the proposed controller for the generated walking gait. The chosen simulation engine is Gazebo executed in a Laptop running Ubuntu 18.04 OS with an Intel Core i7-8750H processor clocked at 2.20GHz with 32GB of RAM. The simulation sets the controller frequency at 1KHz and considers the actuators' torque limits, joints position, and velocity bounds, and only the sensor information available on ATALANTE.

Fig. 4 shows the resulting stable walking gaits for the regulated HZD outputs. Simulations executing HZD without output regulation result in an average of 15 steps before falling. Fig. 5 shows a comparison of the CoM evolution during one gait with respect to the support foot for HZD (not regulated) and HZD with regulation. The regulator action drives the robot CoM back to its nominal path, which under the linear inverted pendulum paradigm, drives the ZMP closer to its designed bounds.

C. Experimental Results

The experiments will be conducted with a 145 lb mannequin securely strapped to the ATALANTE to emulate the situations with a real patient with paraplegia (see Fig. 7.)

Without the dummy, the exoskeleton falls backward because its torso is displaced to allow a user inside. As the dummy is different from the model used in the optimization, it accounts for the typical case of an exoskeleton robot where there is limited information of the user, allowing to transfer the formal method to the real users.

A PD control at 1KHz drives the joint outputs to the designed surface $\mathscr{Z}_\alpha$ or $\mathscr{Z}_\beta$. However, using purely HZD control resulted in unstable walking gaits that required external support for data acquisition.

As proposed, the control method proposed resulted in a stable walking gait, as seen in Fig 6. Fig. 10 plots the tracking performance achieved with the PD controller and Fig. 9 shows the phase portraits of the joints.

Fig. 8 compares the experimental CoM evolution with respect to the support leg for several steps. The color areas show the regions where the CoM evolved during the experiment and indicates as expected that the regulated CoM is closer to the nominal CoM trajectory.

V. CONCLUSIONS

This paper proposes the addition of a regulation term in the virtual-constraints to aid the lateral stability of a bipedal robot through ZMP manipulation. The method was successfully experimented on ATALANTE walking at a speed of 0.05m/s with a dummy with realistic size and weight.

An advantage of the proposed method is that it respects the hybrid invariance property designed for orbit $\mathscr{Z}_\alpha$ by providing a regulation strategy that generates an orbit $\mathscr{Z}_\beta$ that inherits this property.

The primary assumption for the ZMP manipulation relies on the linear inverted pendulum behavior of the lateral movement. However, the current implementation is unable to use a force sensor to measure the ZMP; in consequence, the regulation of the ZMP was performed indirectly through CoM regulation. Having an effective control action for ZMP during the gait increases the robustness exhibited by the
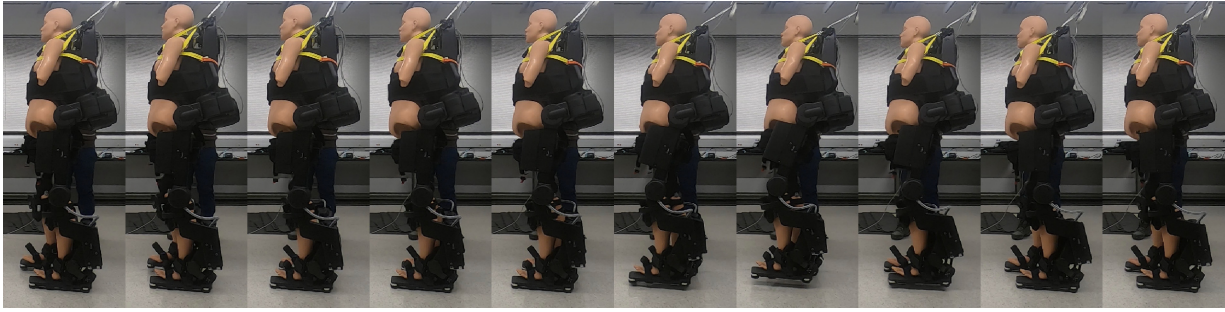
Fig. 6. No regulation for CoM trajectory with respect to the supporting foot. The blue line represents the nominal lateral CoM and the red line the actual CoM trajectory

Fig. 7. Setting of exoskeleton ATALANTE with a mannequin.

Fig. 8. The shaded regions represent the the typicall CoM trajectories for regulated(blue) and unregulated (green) walking. The red dotted line represent the nominal CoM trajectory from the optimization.

robot. Moreover, a similar strategy can be to switch among different walking gaits by making sure that transitioning among them respects the ZMP constraints.

Robust walking gaits and safe transitioning among different orbits provide the possibility of achieving agile and efficient dynamic locomotion for different tasks and allow exoskeletons a step closer to support people with lower-limb paralysis.

REFERENCES

[1] M. Vukobratovic, D. Hristic, and Z. Stojiljkovic, "Development of active anthropomorphic exoskeletons," *Medical and biological engineering*, vol. 12, no. 1, pp. 66–80, 1974.

[2] J. Grundmann and A. Seireg, "Computer control of multi-task exoskeleton for paraplegics," in *Proceedings of the Second CISM/IFTOMM International Symposium on the Theory and Practice of Robots and Manipulators*, 1977, pp. 233–240.

[3] A. M. Dollar and H. Herr, "Lower extremity exoskeletons and active orthoses: challenges and state-of-the-art," *IEEE Transactions on robotics*, vol. 24, no. 1, pp. 144–158, 2008.
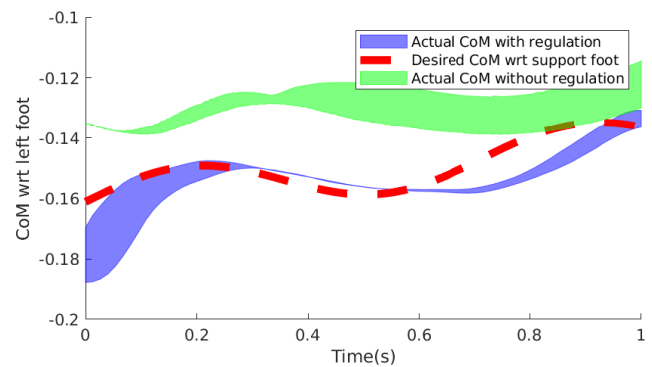
[4] S. Kajita, F. Kanehiro, K. Kaneko, K. Yokoi, and H. Hirukawa, "The 3D linear inverted pendulum model: a simple modeling for a biped walking pattern generation," in *Proceedings of the IEEE/RSJ International Conference on Intelligent Robots and Systems*, 2001, pp. 239–246.

[5] P. M. Wensing and D. E. Orin, "High-speed humanoid running through control with a 3d-slip model," *IEEE/RSJ International Conference on Intelligent Robots and Systems*, pp. 5134–5140, Nov. 2013. [Online]. Available: http://ieeexplore.ieee.org/lpdocs/epic03/wrapper.htm?arnumber=6697099 http://ieeexplore.ieee.org/xpls/abs_all.jsp?arnumber=6697099

[6] T. Sugihara and Y. Nakamura, "Contact phase invariant control for humanoid robot based on variable impedant inverted pendulum model," in *2003 IEEE International Conference on Robotics and Automation (Cat. No. 03CH37422)*, vol. 1. IEEE, 2003, pp. 51–56.

[7] A. D. Ames, "First steps toward underactuated human-inspired bipedal robotic walking," in *2012 IEEE International Conference on Robotics and Automation (ICRA)*, May 2012, pp. 1011–1017.

[8] A. D. Kuo, "Stabilization of lateral motion in passive dynamic walking," *The International Journal of Robotics Research*, vol. 18, no. 9, pp. 917–930, 1999. [Online]. Available: http://dx.doi.org/10.1177/02783649922066655

[9] S. Kuindersma, R. Deits, M. Fallon, A. Valenzuela, H. Dai, F. Permenter, T. Koolen, P. Marion, and R. Tedrake, "Optimization-based locomotion planning, estimation, and control design for the Atlas humanoid robot," *Autonomous Robots*, vol. 40, no. 3, pp. 429–455, Mar. 2016. [Online]. Available: http://dx.doi.org/10.1007/s10514-015-9479-3

[10] S. Kajita, F. Kanehiro, K. Kaneko, K. Fujiwara, K. Harada, K. Yokoi, and H. Hirukawa, "Biped walking pattern generation by using preview control of zero-moment point," in *IEEE International Conference on*
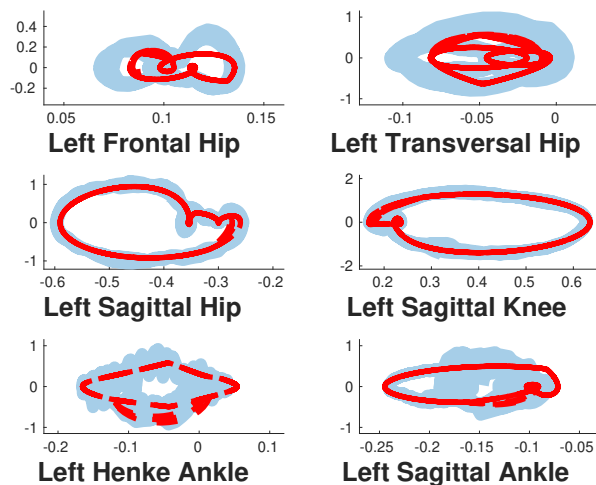
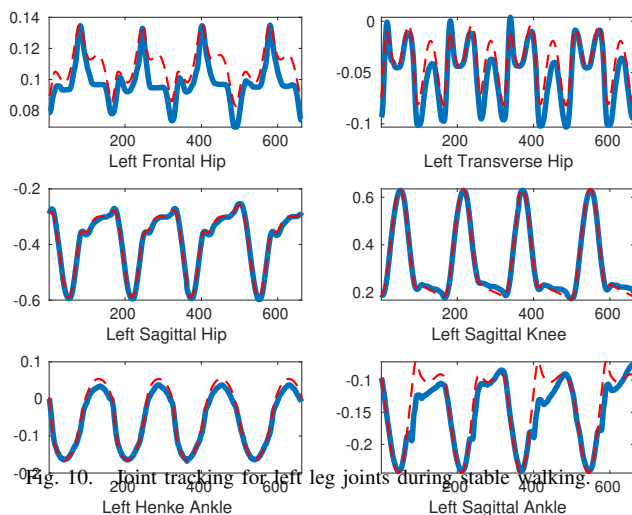Fig. 9.   Phase portrait of the left leg joints during stable walking.

Fig. 10.   Joint tracking for left leg joints during stable walking.

Robotics and Automation, vol. 2, Sep. 2003, pp. 1620–1626.

[11] J. Park and Y. Youm, "General zmp preview control for bipedal walking," in *Proceedings 2007 IEEE International Conference on Robotics and Automation*.   IEEE, 2007, pp. 2682–2687.

[12] J. Pratt, T. Koolen, T. de Boer, J. Rebula, S. Cotton, J. Carff, M. Johnson, and P. Neuhaus, "Capturability-based analysis and control of legged locomotion, part 2: application to m2v2, a lower-body humanoid," *The International Journal of Robotics Research*, vol. 31, no. 10, pp. 1117–1133, Aug. 2012. [Online]. Available: http://ijr.sagepub.com/cgi/doi/10.1177/0278364912452762

[13] S. Collins, A. Ruina, R. Tedrake, and M. Wisse, "Efficient bipedal robots based on passive-dynamic walkers," *Science*, vol. 307, no. 5712, pp. 1082–1085, 2005.

[14] E. R. Westervelt, J. W. Grizzle, C. Chevallereau, J. H. Choi, and B. Morris, *Feedback control of dynamic bipedal robot locomotion*. CRC press Boca Raton, 2007.

[15] A. Hereid and A. D. Ames, "FROST: fast robot optimization and simulation toolkit," in *Proc. IEEE/RSJ Int. Conf. Intelligent Robots and Systems (IROS)*.   Vancouver, BC, Canada: IEEE/RSJ, Sep. 2017, pp. 719–726.

[16] A. Hereid, C. M. Hubicki, E. A. Cousineau, and A. D. Ames, "Dynamic humanoid locomotion: a scalable formulation for HZD gait optimization," *IEEE Transactions on Robotics*, vol. 34, no. 2, pp. 370–387, Apr. 2018.

[17] X. Da, O. Harib, R. Hartley, B. Griffin, and J. W. Grizzle, "From 2D design of underactuated bipedal gaits to 3D implementation: Walking with speed tracking," *IEEE Access*, vol. 4, pp. 3469–3478, 2016.

[18] S. Rezazadeh, C. Hubicki, M. Jones, A. Peekema, J. Van Why, A. Abate, and J. Hurst, "Spring-mass walking with ATRIAS in 3D: Robust gait control spanning zero to 4.3 kph on a heavily underactuated bipedal robot," in *ASME 2015 Dynamic Systems and Control Conference*.   American Society of Mechanical Engineers, 2015, pp. V001T04A003–V001T04A003.

[19] S. Veer and I. Poulakakis, "Safe adaptive switching among dynamical movement primitives: Application to 3d limit-cycle walkers," in *2019 International Conference on Robotics and Automation (ICRA)*.   IEEE, 2019, pp. 3719–3725.

[20] X. Da and J. Grizzle, "Combining trajectory optimization, supervised machine learning, and model structure for mitigating the curse of dimensionality in the control of bipedal robots," *The International Journal of Robotics Research*, vol. 38, no. 9, pp. 1063–1097, jul 2019. [Online]. Available: https://doi.org/10.1177/0278364919859425

[21] S. Veer, M. S. Motahar, and I. Poulakakis, "Generation of and switching among limit-cycle bipedal walking gaits," in *2017 IEEE 56th Annual Conference on Decision and Control (CDC)*.   IEEE, 2017, pp. 5827–5832.

[22] E. R. Westervelt, J. W. Grizzle, and C. C. De Wit, "Switching and pi control of walking motions of planar biped walkers," *IEEE Transactions on Automatic Control*, vol. 48, no. 2, pp. 308–312, 2003.

[23] O. Harib, A. Hereid, A. Agrawal, T. Gurriet, S. Finet, G. Boeris, A. Duburcq, M. E. Mungai, M. Masselin, A. D. Ames, K. Sreenath, and J. Grizzle, "Feedback control of an exoskeleton for paraplegics: toward robustly stable hands-free dynamic walking," *IEEE Control System Maganize*, vol. 38, no. 6, pp. 61–87, Dec. 2018.

[24] T. Gurriet, S. Finet, G. Boeris, A. Duburcq, A. Hereid, O. Harib, M. Masselin, J. Grizzle, and A. D. Ames, "Towards restoring locomotion for paraplegics: realizing dynamically stable walking on exoskeletons," in *2018 IEEE International Conference on Robotics and Automation (ICRA)*, May 2018, pp. 2804–2811.